ACES On-orbit Commissioning: Preliminary Results

Luigi Cacciapuoti

3rd Terrestrial Very-Long-Baseline Atom Interferometry Meeting
Leibniz University- Hannover, Germany

20-22 August 2025

ACES mission

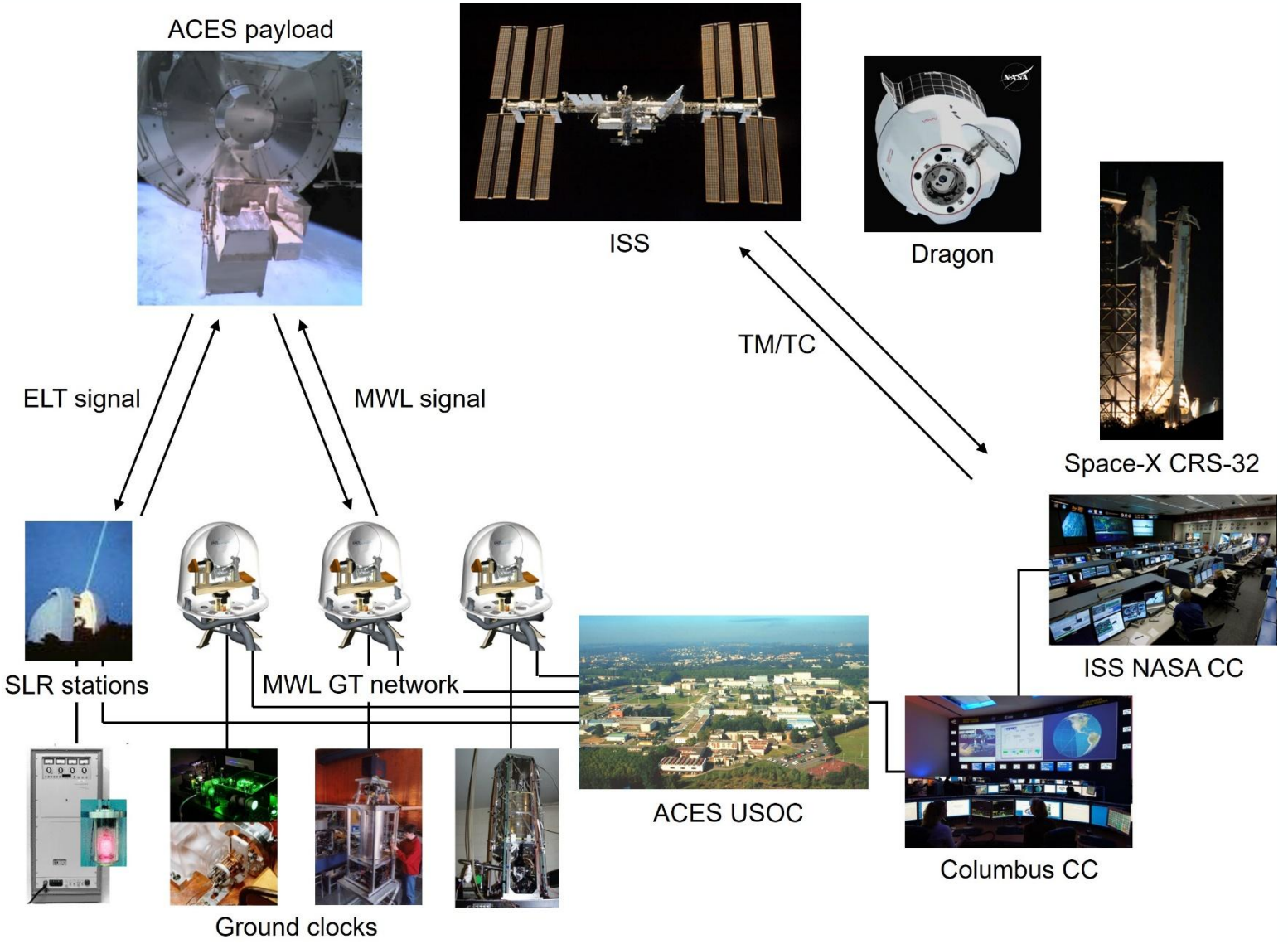

ACES launch: 21 April 2025

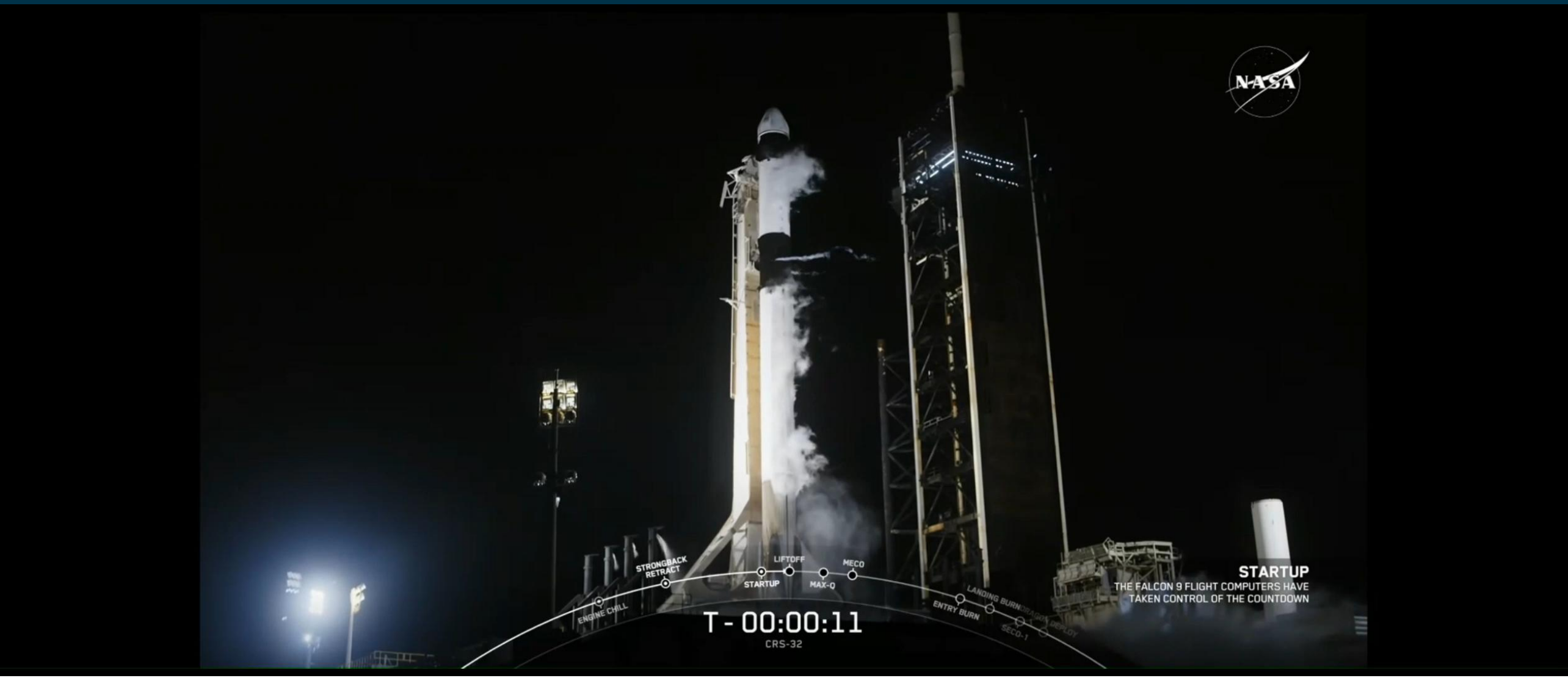

Credits NASA-ESA

ACES robotic operation: 25 April 2025

Credits NASA-ESA

The ACES payload

- **PHARAO** (CNES): Atomic clock based on laser cooled Cs atoms
- **SHM**: Active hydrogen maser
- **FCDP**: Clocks comparison and distribution
- **MWL**: T&F transfer link
- **GNSS** receiver
- **ELT**: Optical link
- **Support subsystems**
  - **XPLC**: External PL computer
  - **PDU**: Power distribution unit,
  - Mechanical, thermal subsystems
  - **CEPA**: Columbus External PL Adapter

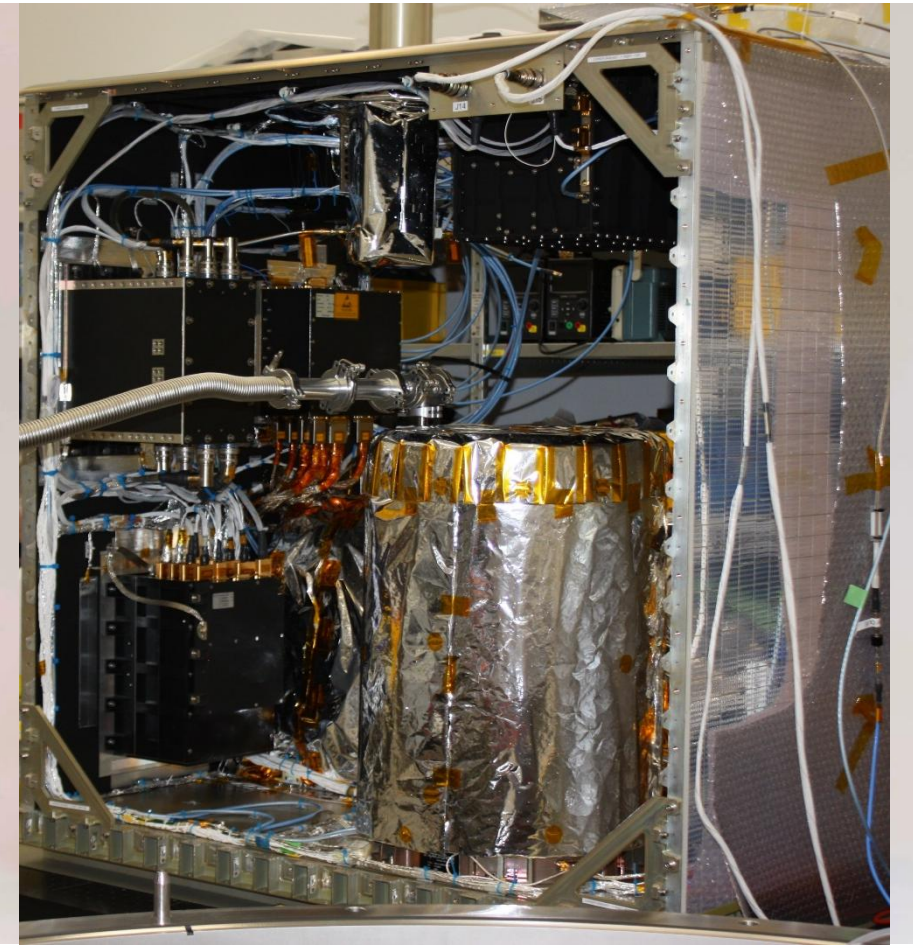

Volume: 1172x867x1246 mm^3
Mass: 240 kg (w/o CEPA)
Power: 600 W

Atomic Clock Ensemble in Space

Science

ACES – Fundamental Physics tests

ACES Mission Objectives	ACES performances	Scientific background and recent results
Gravitational red-shift	Absolute measurement of the gravitational red-shift to $< 2 \cdot 10^{-6}$ after 10 days of integration time, after having validated PHARAO accuracy.	Factor 70 improvement over the GPA experiment and factor 10 over tests involving Galileo 5 and 6 satellites.
Time drifts of fundamental constants	Time variations of α constrained to $\alpha^{-1} \cdot d\alpha/dt < 3 \cdot 10^{-18}$ yr $^{-1}$ after 3 years of mission.	Comparisons of clocks based on different atoms and atomic transitions on a worldwide scale to constrain α, m_e/Λ_{QCD} and m_q/Λ_{QCD}.
Dark matter search with atomic clocks	Establish bounds on topological dark matter models based on the comparisons of clocks in the ACES network.	Comparisons via the ACES network imposing limits on the three coupling constants Λ_α, Λ_e, and Λ_q in the model Lagrangian. Measurements over an interval T between encounters of 20 d. Simultaneous observation with several clocks along different baselines providing ways to confirm any observation above the sensitivity threshold and control the measurement systematics. Screening effect on the dark matter field due to the Earth mass reduced to about 0.06 on the space clock PHARAO with respect to ground clocks (~ 10^{-7}).

Gravitational redshift test

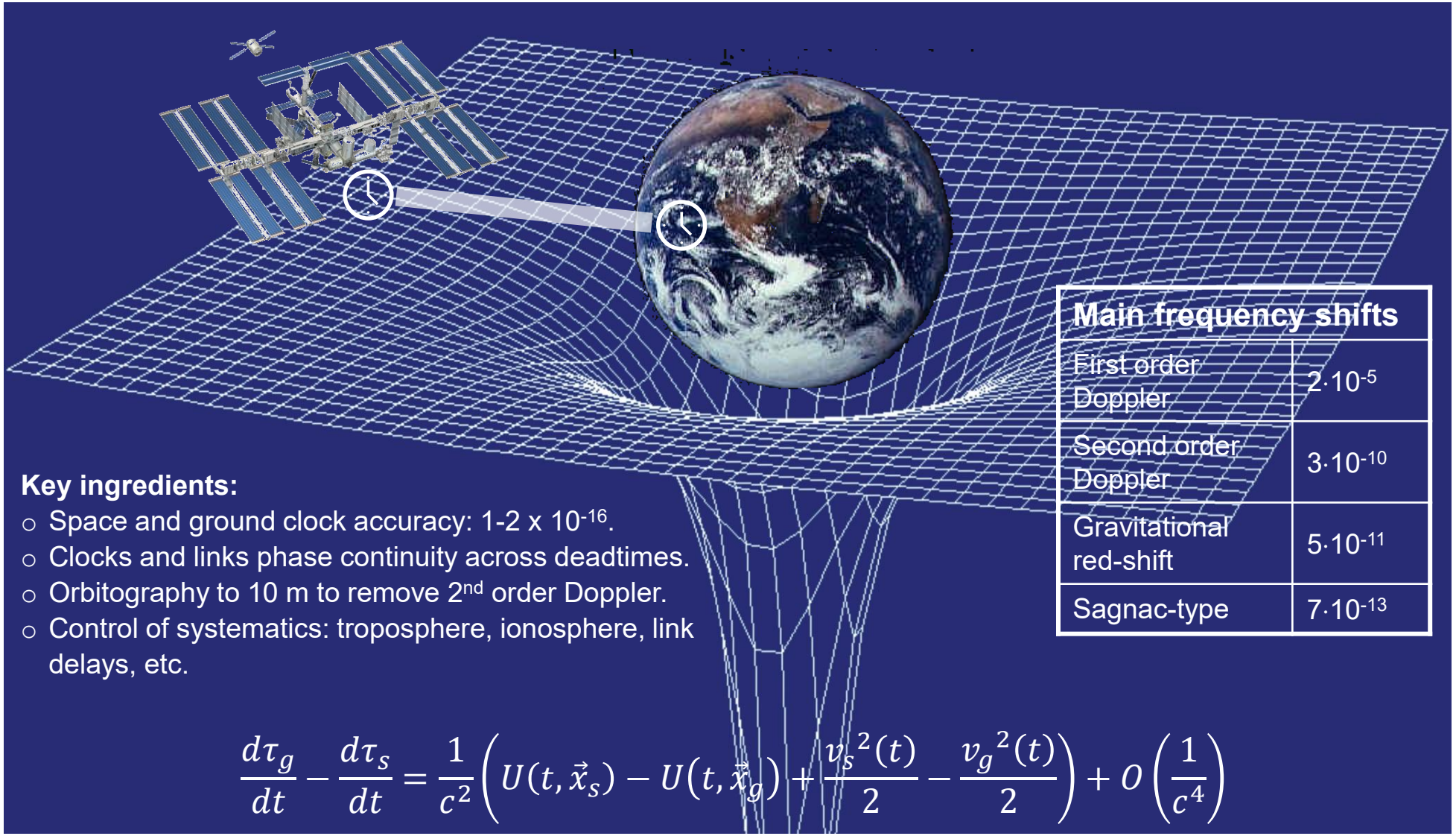

Key ingredients:

- Space and ground clock accuracy: 1-2 x 10^{-16}.
- Clocks and links phase continuity across deadtimes.
- Orbitography to 10 m to remove 2nd order Doppler.
- Control of systematics: troposphere, ionosphere, link delays, etc.

Main frequency shifts	
First order Doppler	$2 \cdot 10^{-5}$
Second order Doppler	$3 \cdot 10^{-10}$
Gravitational red-shift	$5 \cdot 10^{-11}$
Sagnac-type	$7 \cdot 10^{-13}$

$$\frac{d\tau_g}{dt} - \frac{d\tau_s}{dt} = \frac{1}{c^2}\left(U(t,\vec{x}_s) - U(t,\vec{x}_g) + \frac{{v_s}^2(t)}{2} - \frac{{v_g}^2(t)}{2}\right) + O\left(\frac{1}{c^4}\right)$$

ACES – Scientific applications

Relativistic geodesy

- Relativistic geodesy: measurement of geopotential differences based on the red-shift measured between two clocks at two different locations.
- ACES intercontinental comparisons of optical clocks at the 10^{-17} level after 4 days, corresponding to a resolution on the local height above the geoid at the 10 cm level.
- The global coverage offered by ACES will complement the results of the CHAMP, GRACE, and GOCE missions.

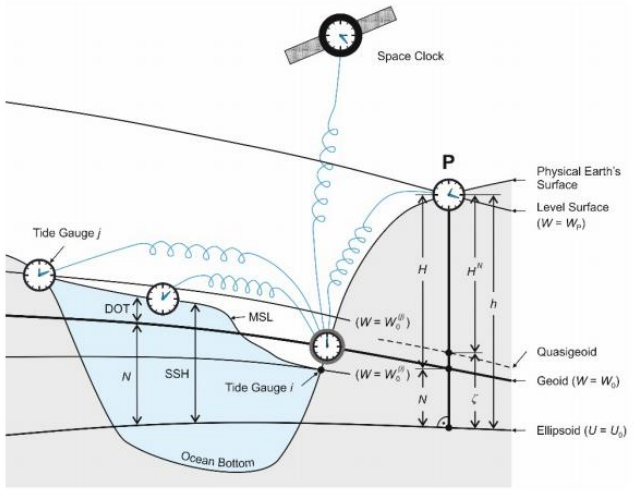

Rep. Prog. Phys. 81, 064401 (2018)

Clocks synchronization

- MWL and ELT clocks synchronization at the 100 ps and 50 ps level, respectively.

Atomic time scales (TAI)

- The PHARAO clock is accurate to $1\text{-}2 \cdot 10^{-16}$.
- MWL will provide means to compare atomic clocks on a worldwide scale:
  - PHARAO and primary standards on ground contributing to TAI.
  - Optical clock comparisons to $1 \cdot 10^{-17}$ will help SI second redefinition.

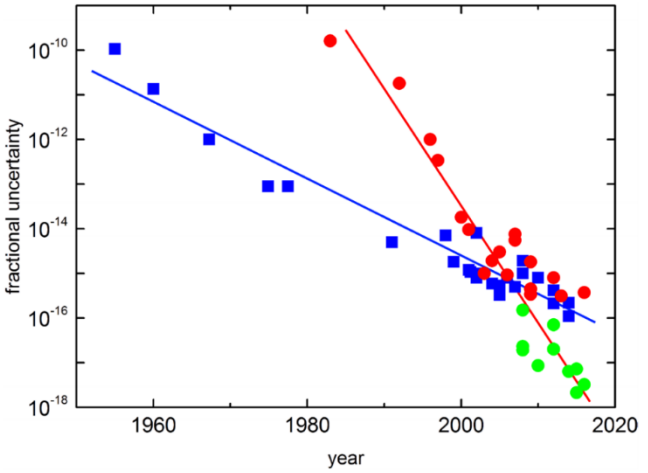

Metrologia 55, 188 (2018)

Atomic Clock Ensemble in Space

In-orbit status

The PHARAO clock

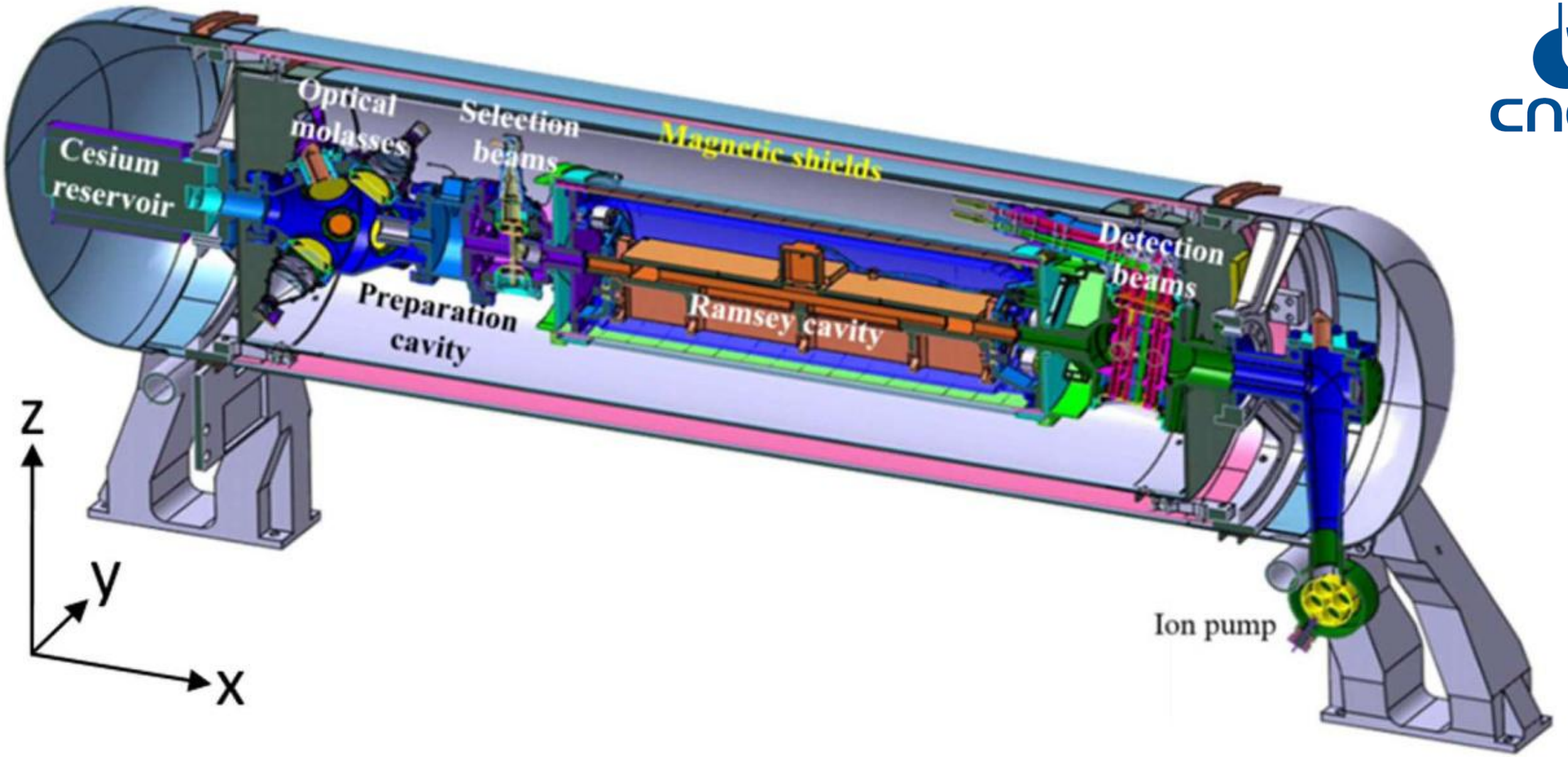

Metrologia **57** (2020) 055005

PHARAO Ramsey fringes I

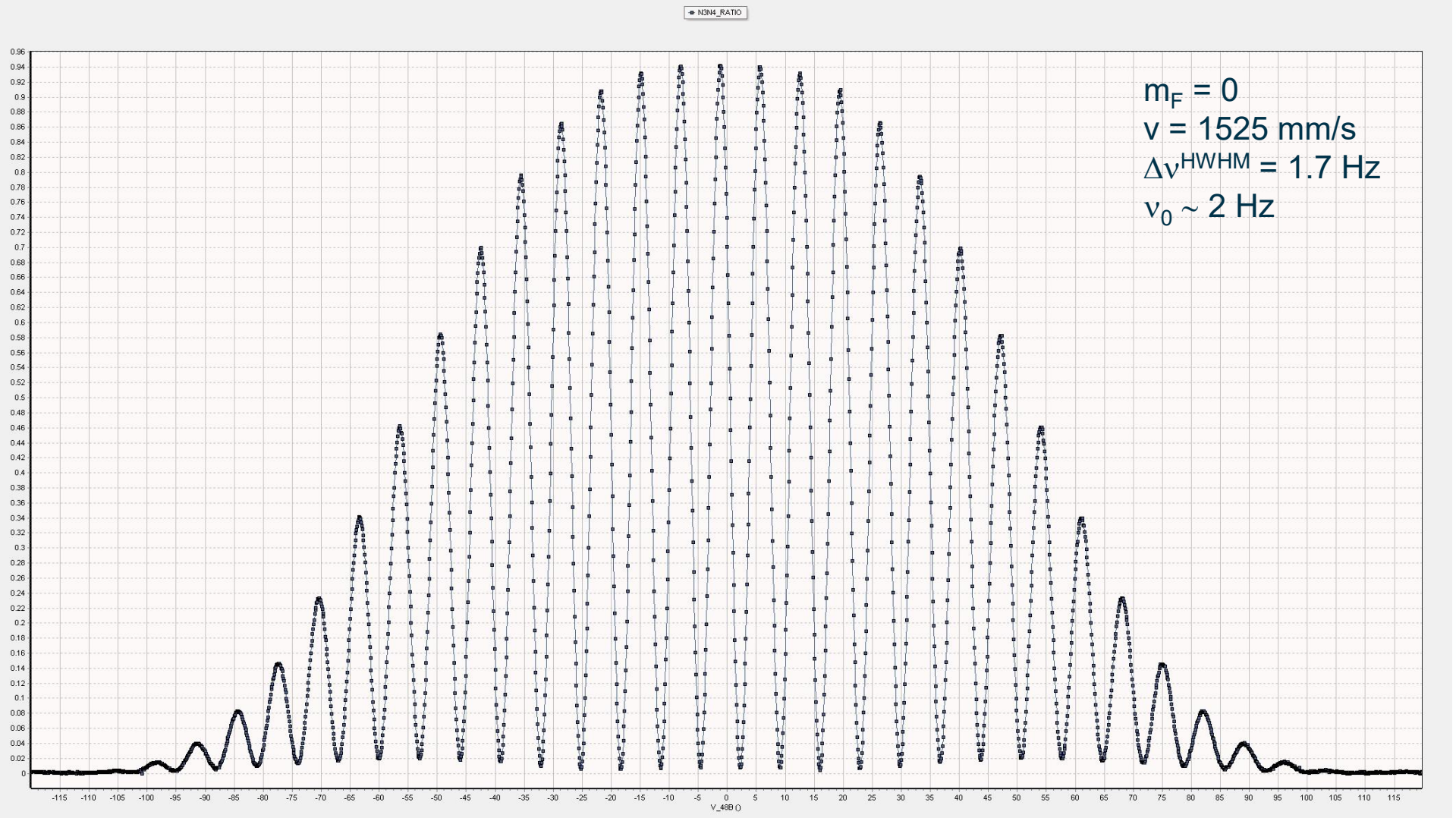

PhL, LTE/CNES, ESA, OP, LNE, PSL, SU

PHARAO Ramsey fringes II

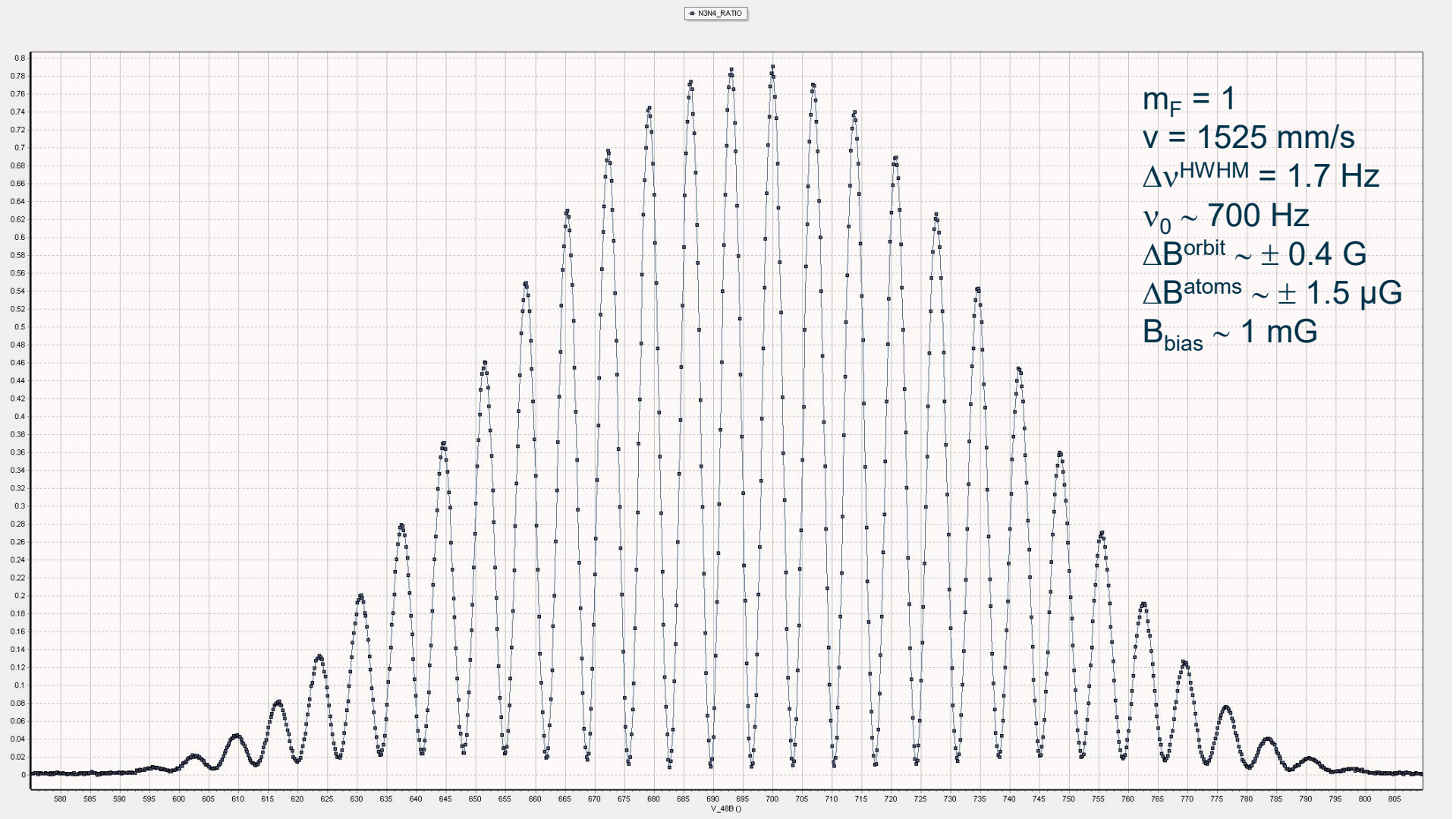

PhL, LTE/CNES, ESA, OP, LNE, PSL, SU

PHARAO Ramsey fringes III

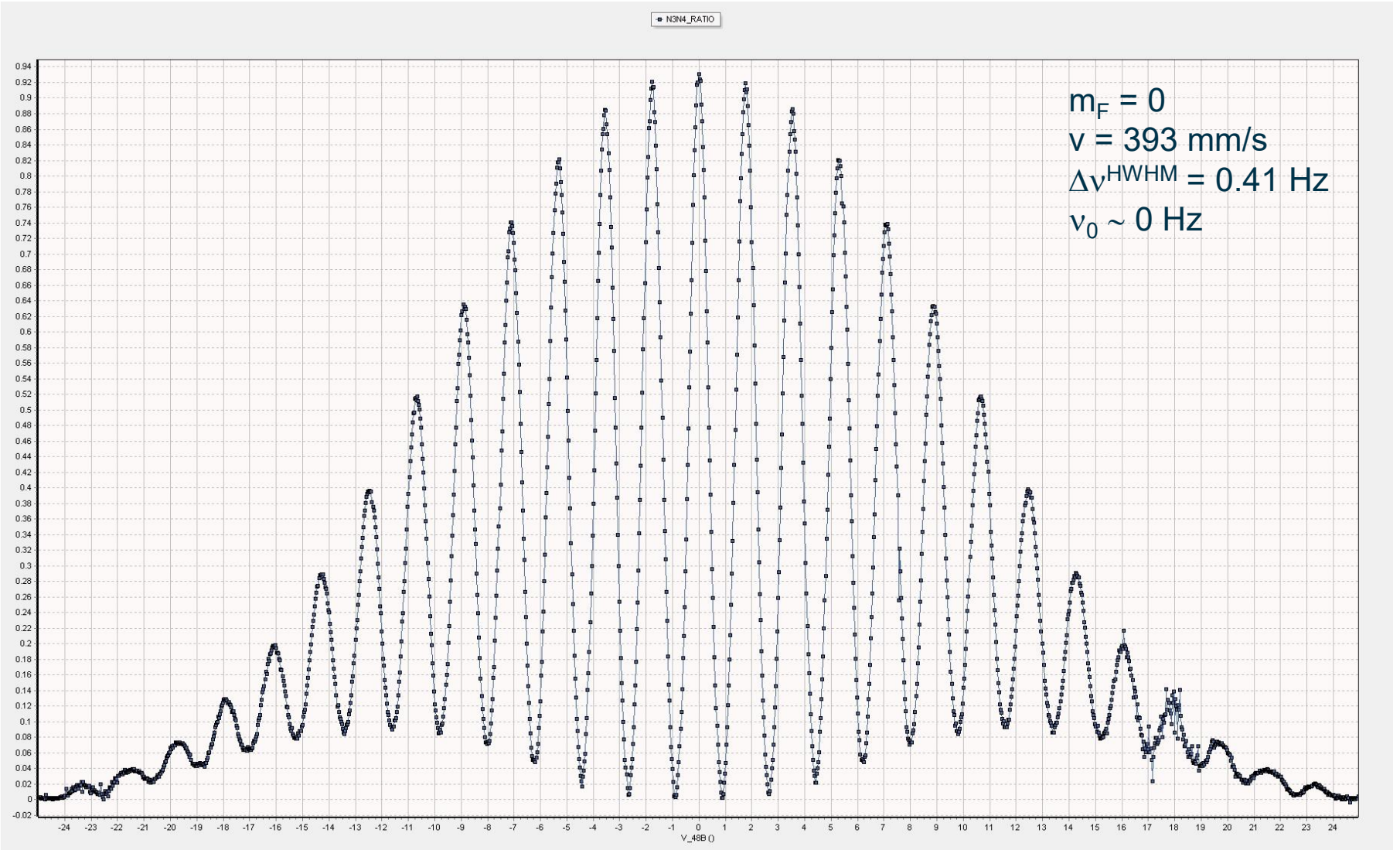

PhL, LTE/CNES, ESA, OP, LNE, PSL, SU

PHARAO Ramsey fringes IV

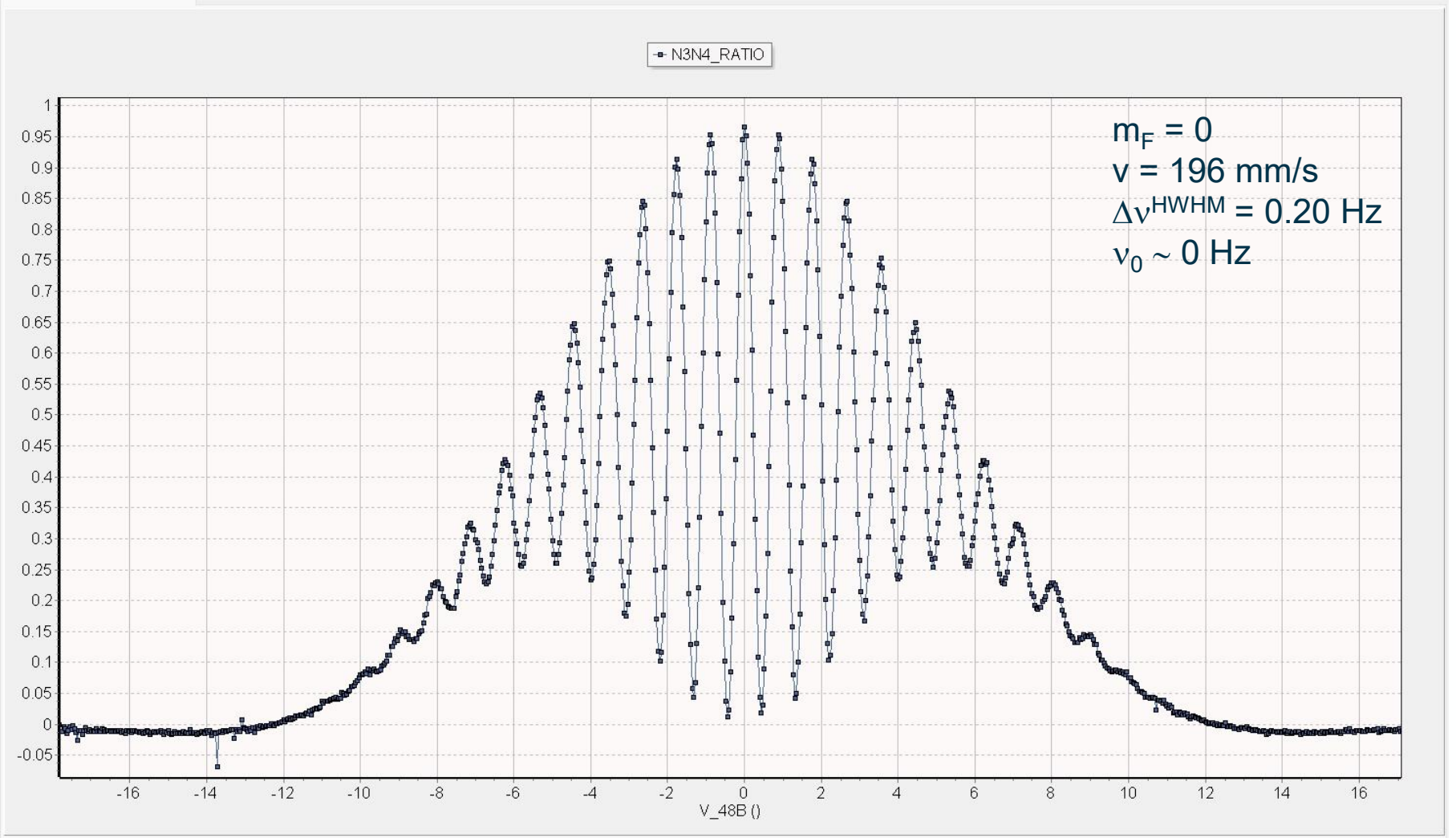

PhL, LTE/CNES, ESA, OP, LNE, PSL, SU

MWL

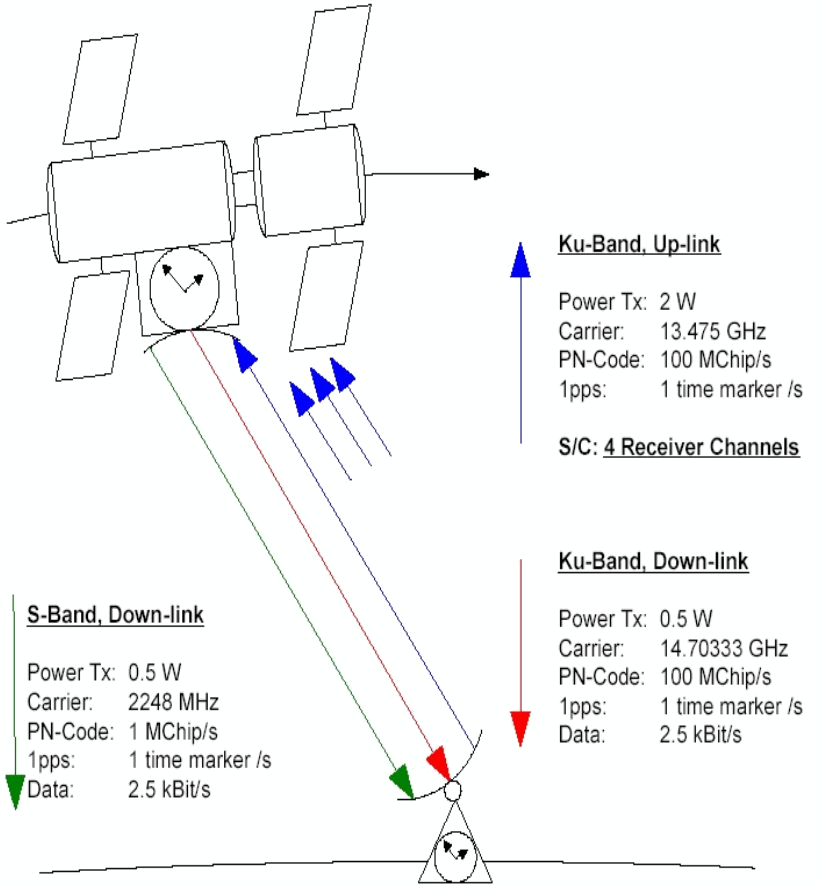

AIRBUS DEFENCE & SPACE TIMETECH TZR EREMS

- Two-way link:
  - Removal of the troposphere time delay (8.3-103 ns).
  - Removal of 1st order Doppler effect.
  - Removal of instrumental delays and common mode effects.
- Additional down-link in the S-band:
  - Determination of the ionosphere TEC.
  - Correction of the ionosphere time delay (0.3-40 ns in S-band, 6-810 ps in Ku-band).
- Phase PN code modulation: Removal of 2π phase ambiguity.
- High chip rate (100 MChip/s) on the code:
  - Higher resolution.
  - Multipath suppression.
- Carrier and code phase measurements (80 ms sampling time).
- Data link: 2 kBits/s on the S-band down-link to obtain clock comparison results in real time.
- Up to 4 simultaneous space-to-ground clock comparisons

MWL measurements and scientific products

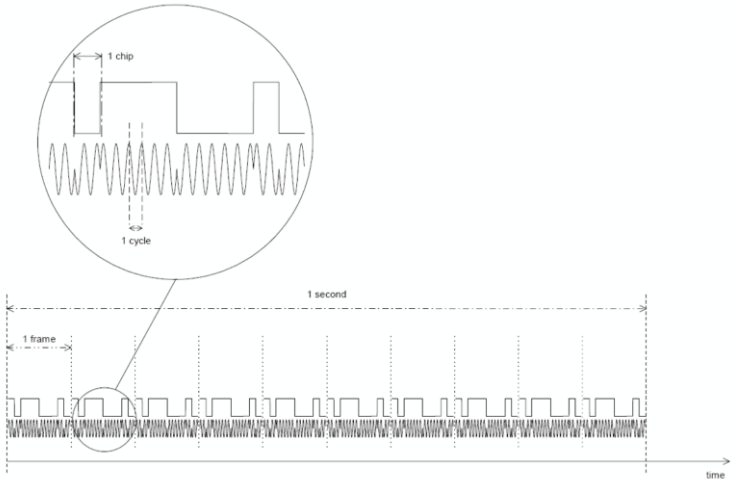

Code and carrier phase measurements on Ku-band up/down-link

$$\Delta\tau^s\left(\tau^s(t_2^o)\right) = Des(t_2^o) - \left[[\Delta_{T1}^g]^t + T_{12} + [\Delta_{R1}^s]^t\right]^g \qquad \Delta\tau^g\left(\tau^g(t_4^o)\right) = -Des(t_4^o) - \left[[\Delta_{T2}^s]^t + T_{34} + [\Delta_{R2}^g]^t\right]^s$$

and S-band down-link

$$\Delta\tau^g\left(\tau^g(t_6^o)\right) = -Des(t_6^o) - \left[[\Delta_{T3}^s]^t + T_{56} + [\Delta_{R3}^g]^t\right]^s$$

where

$$T_{12} = \frac{R_{12}}{c} + \frac{2GM_E}{c^3}\ln\left(\frac{x_g(t_1)+x_s(t_2)+R_{12}}{x_g(t_1)+x_s(t_2)-R_{12}}\right) + \Delta_{12}^{tropo} + \Delta_{12}^{iono} + O(\frac{1}{c^4})$$

$$T_{34} = \frac{R_{34}}{c} + \frac{2GM_E}{c^3}\ln\left(\frac{x_g(t_4)+x_s(t_3)+R_{34}}{x_g(t_4)+x_s(t_3)-R_{34}}\right) + \Delta_{34}^{tropo} + \Delta_{34}^{iono} + O(\frac{1}{c^4})$$

$$T_{56} = \frac{R_{56}}{c} + \frac{2GM_E}{c^3}\ln\left(\frac{x_g(t_6)+x_s(t_5)+R_{56}}{x_g(t_6)+x_s(t_5)-R_{56}}\right) + \Delta_{56}^{tropo} + \Delta_{56}^{iono} + O(\frac{1}{c^4})$$

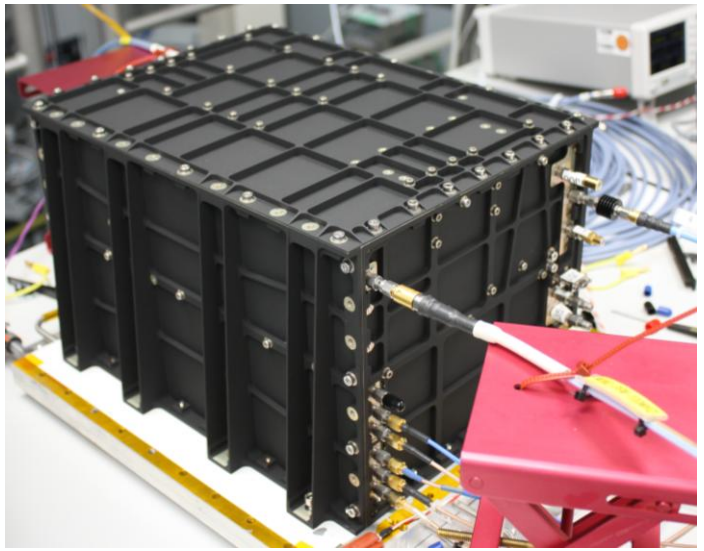

Scientific Products		**…from**
Space-to-ground Desynchronization	$\tau^g(t_a) - \tau^s(t_a)$	$\Delta\tau^s\left(\tau^s(t_2^o)\right) - \Delta\tau^g\left(\tau^g(t_4^o)\right)$
Ionosphere Total Electron Content	$(\frac{1}{f_3^2} - \frac{1}{f_2^2})\frac{40.308}{c}C_e$	$\Delta\tau^g(\tau^g(t_4^o)) - \Delta\tau^g(\tau^g(t_6^o))$
Range + Tropospheric Delay	$D(t_4)$ & Δ_{34}^{tropo}	$\Delta\tau^s\left(\tau^s(t_2^o)\right) + \Delta\tau^g(\tau^g(t_4^o))$

MWL – First space-to-ground link above LTE (Paris)

Space transceiver
MWL PFM @ ISS

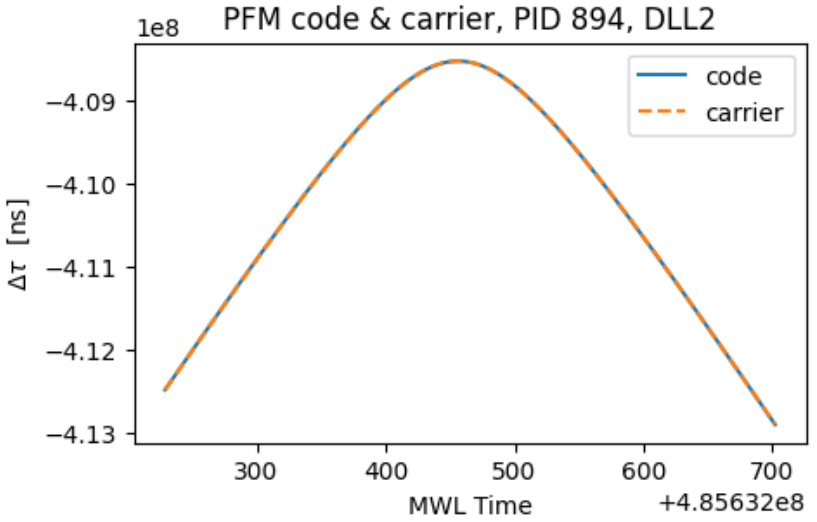

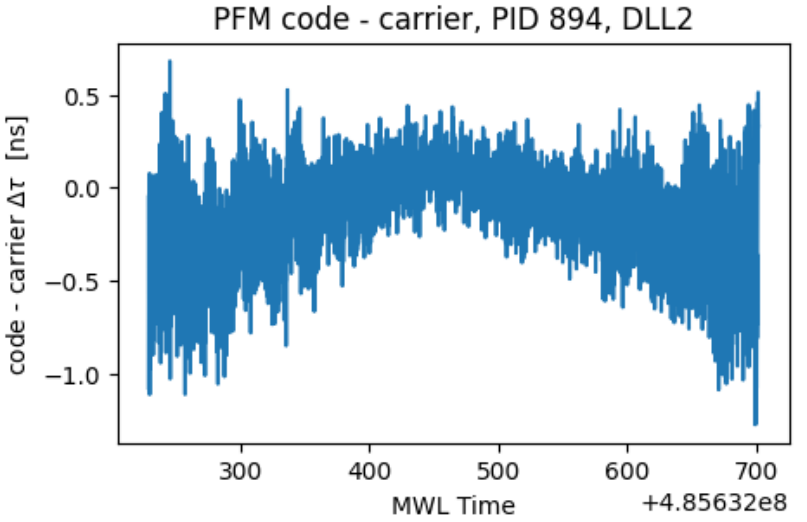

Ground transceiver
GT#101 @ LTE

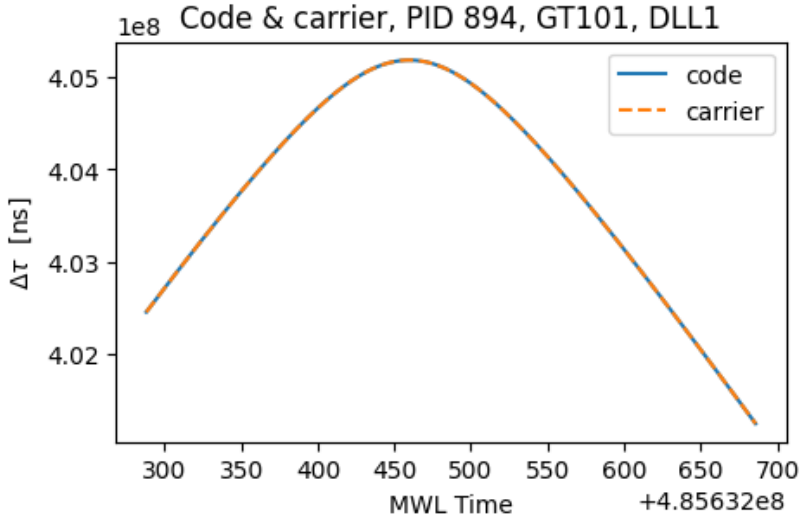

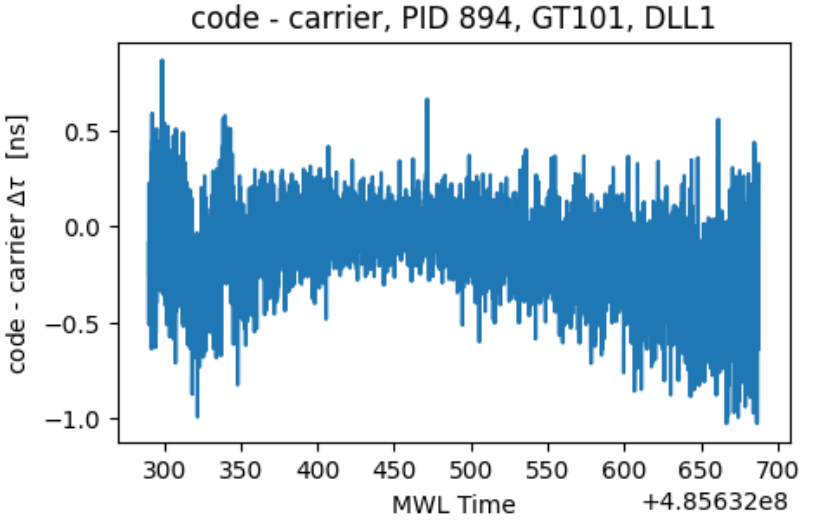

MWL GT code phase performance on a dynamic pass

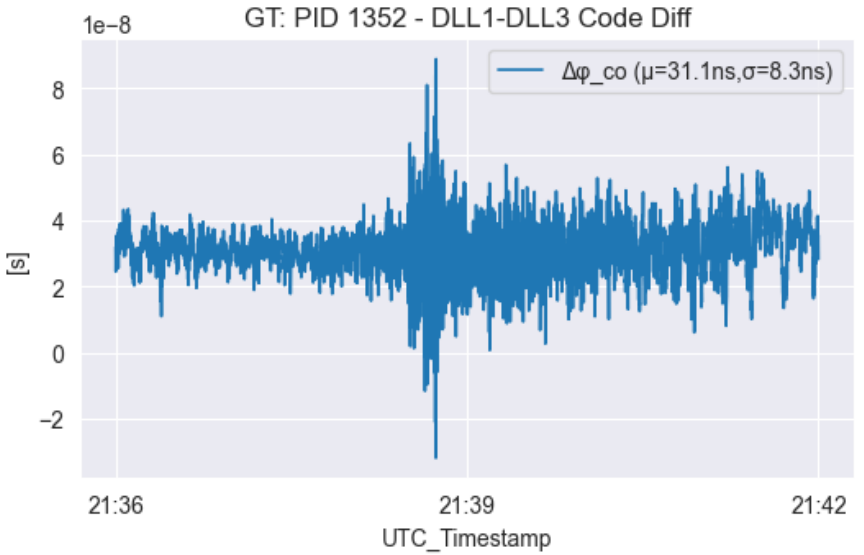

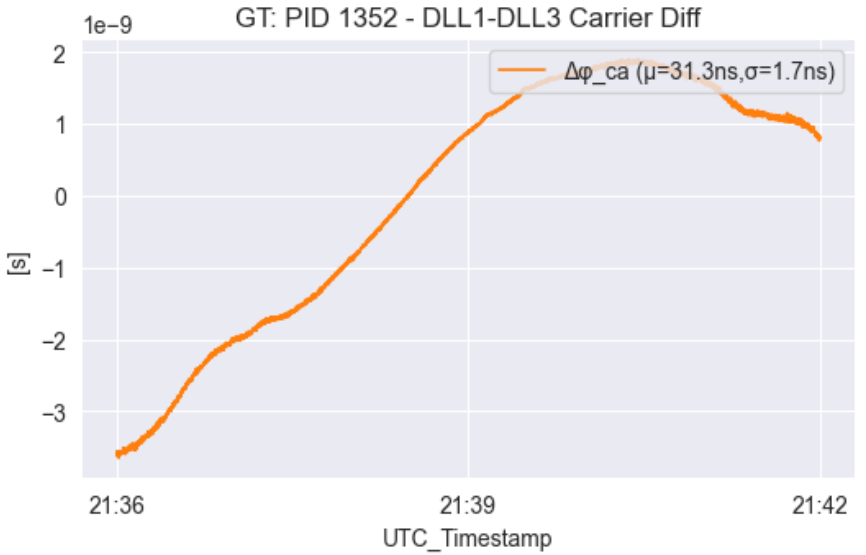

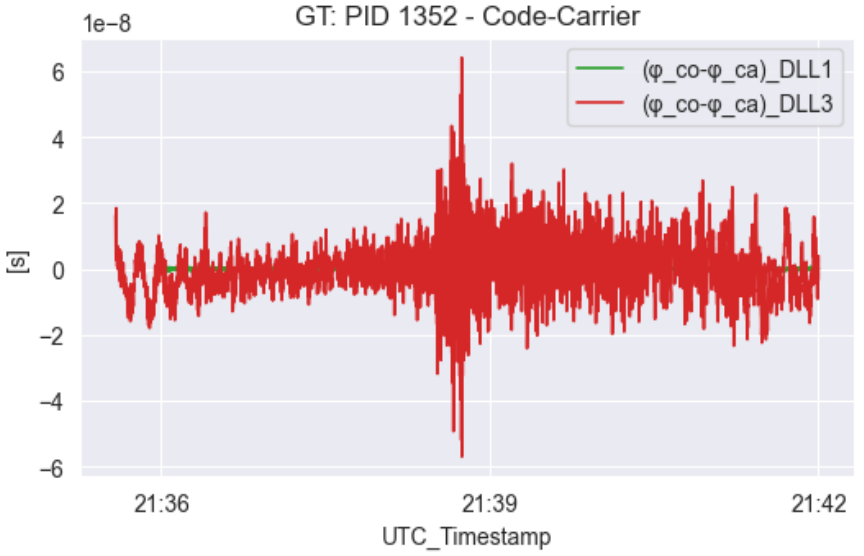

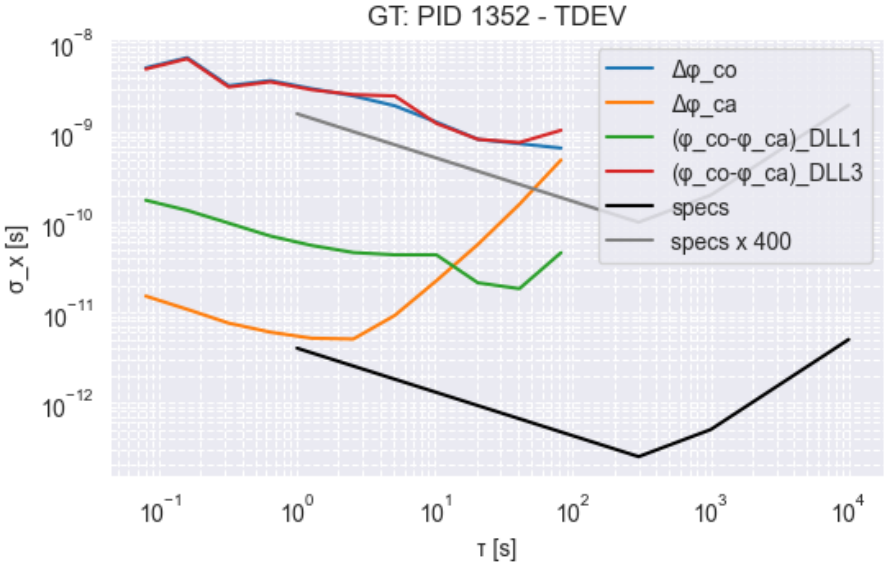

Corrections

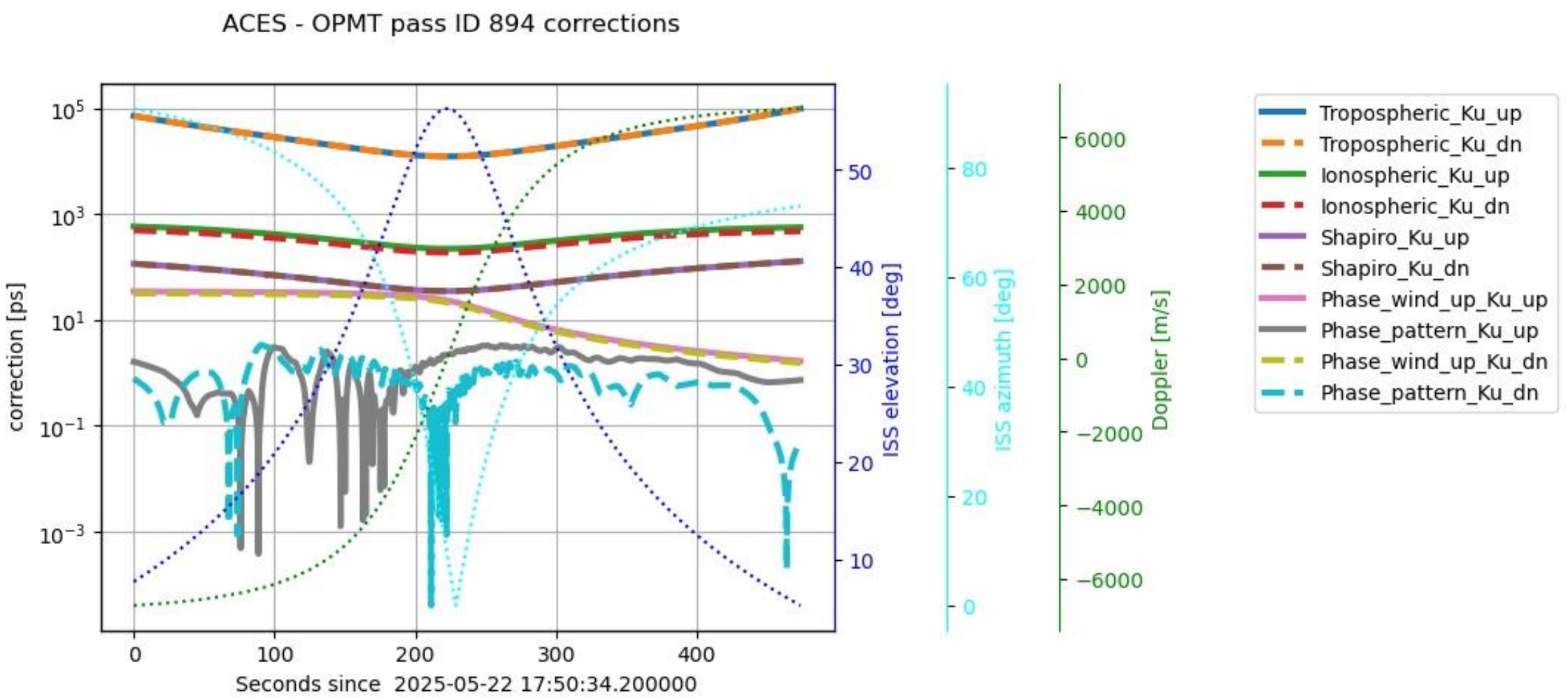

ACES MWL network

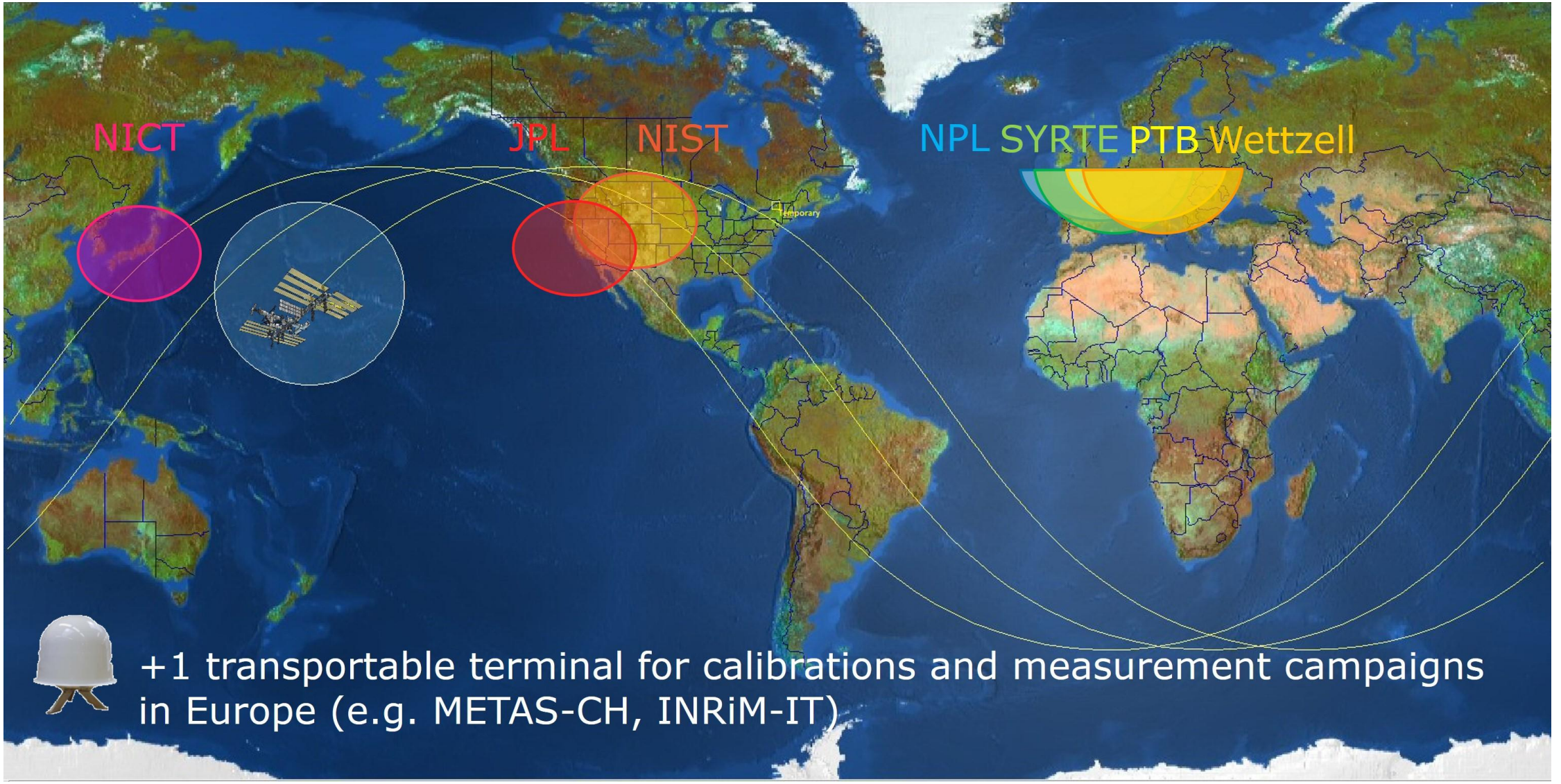

Atomic Clock Ensemble in Space

Summary and outlook

Next steps

- PHARAO clock is operating correctly, following the expected behaviour:
  - Sub-Hz linewidths recorded at 393 mm/s and 196 mm/s launch velocity.
  - Further optimization ongoing.
- SHM clock is showing an anomalous behaviour. No atomic signal could be detected so far.
- MWL space-to-ground links established:
  - Ku-band performance in line with expectation.
  - S-band performance to be improved for iono correction.
  - More work is needed to ensure reliable operation of the MWL GTs.
- Commissioning activities are progressing. They include:
  - Characterization of the clocks' stability and accuracy:
  - Evaluation of MWL and ELT in space:
    - Common clock comparisons with two co-located MWL GTs.
    - Common view comparisons with two MWL GTs and OGSs.
    - Common clock comparisons with co-located MWL GT and OGS.
- Commission activities will continue until end October 2025 to release ACES for the routine science phase.

L. Cacciapuoti[1], S. Pataraia[1], T. Peignier[1], T. Plumaris[1], S. Weinberg[1], U. Bishoff[2], P. Crescence[2], A. Helm[2], J. Kehrer[2],, R. Lachaud[2], D. Mitschke[2], T. Niedermaier[2], F.X. Esnault[3], B. Léger[3], E. Thulliez[3],D. Massonnet[3], D. Goujon[4], J. Pittet[4], A. Perri[4], Q. Wang[4], P. Rochat[4], S. Liu[5], W. Schaefer[5], T. Schwall[5], I. Prochazka[6], A. Schlicht[7], U. Schreiber[7], P. Laurent[8], M. Lilley[8], J. Rose[8], P. Wolf[8], K. Gibble[9], C. Salomon[10]

[1]*European Space Agency, ESTEC, Noordwijk, The Netherlands*
[2]*Airbus Defence and Space, Friedrichshafen, Germany*
[3]*CNES, Toulouse, France*
[4]*Orolia Switzerland (Spectratime), Neuchâtel, Switzerland*
[5]*Timetech, Stuttgart, Germany*
[6]*Czech Technical University in Prague, Prague, Czech Republic*
[7]*Technical University of Munich, Munich, Germany*
[8]*SYRTE, Observatoire de Paris-PSL, CNRS, Sorbonne Université, LNE, Paris, France*
[9]*The Pennsylvania State University, University Park, USA*
[10]*Laboratoire Kastler Brossel, ENS, Paris, France*